Effects of nanoparticles on plasma shielding at pulsed laser ablation of metal targets

Alexey N. Volkov*a, Michael A. Stokesa
a Department of Mechanical Engineering, University of Alabama, 7th Avenue, Tuscaloosa, AL
35487, USA

ABSTRACT

In high-power pulsed laser ablation of metals, the material removal usually occurs in the regime of volumetric boiling, when the ablated materials form two-phase plasma plumes composed of neutral atoms, ions, electrons, and a large fraction of nanoparticles/clusters. To predict the effect of plasma shielding induced by absorption of laser radiation in such two-phase plumes, a hybrid multi-phase computational model is developed. The model includes a thermal model of the irradiated target, a model of non-equilibrium ionization of gaseous plasma plume based on the collision-radiation plasma model, and a kinetic equation that describes the distribution of cluster sizes and temperatures. The model accounts for the fragmentation of the target material in the regime of volumetric boiling, evaporation and condensation of nanoparticles, as well as radiation absorption and scattering by all constituents of the plume. The model is used to evaluate the contributions of various factors on the degree of plasma shielding at laser ablation of a copper target irradiated by a nanosecond laser pulse. The simulations show that the radiation scattering by nanoparticles is the dominant mechanism of radiation attenuation. The cluster evaporation and attenuation of laser radiation by nanoparticles are found to have a strong effect on plume dynamics and plasma shielding.

Keywords: Laser ablation, volumetric boiling, two-phase plasma plume, clusters, plasma shielding, collision-radiation model.

1. INTRODUCTION

Pulsed laser ablation of a metal target is the process of material removal induced by the heating of the target by high-power pulses of laser radiation. When the target temperature approaches the thermodynamic critical temperature, the material removal occurs in the regime of volumetric boiling, e.g., [1-3], and the ablation products represent the two-phase mixture of the atomic component and large clusters/nanodroplets. The regime of volumetric boiling is the most relevant regime for industrial applications of laser ablation. The plume of ablation products can absorb the incident laser radiation. The radiation absorption induces ionization of the ablated material. The attenuation of the laser radiation due to its absorption in the plasma plume is often referred to as the plasma shielding effect [4]. In the two-phase laser-induced plumes, the attenuation of laser radiation is caused by both the absorption of laser energy by ions and electrons through photoionization and inverse bremsstrahlung as well as through absorption and scattering of laser radiation by clusters [5].

In the case of ablation by nanosecond pulses of laser radiation, the experiments have shown that the volumetric boiling and strong absorption of laser radiation by the plasma plume usually have threshold fluences that are close to each other and, therefore, both processes usually occur simultaneously [6]. Molecular dynamics simulations of laser ablation induced by ultrashort laser pulses show that, in the regime of volumetric boiling (or phase explosion), the mass fraction of the atomic component in the ablation products can be as small as 3% and the remaining ablated mass is composed of relatively large nanodroplets [7]. At the same time, the experiments on the plasma plume expansion induced by nanosecond pulses revealed large abundances of atoms and ions, e.g., [8]. These facts suggest a strong mass and energy exchange between the atomic components and clusters in the two-phase plumes, which can significantly change the dynamic plume properties and affect the degree of plasma shielding. The effect of cluster-plasma interaction on the plume dynamics can be even stronger in the case of multi-pulse (burst) ablation with high-repetition rate laser pulses [9,10]. The dynamics of the mass and energy exchange between atomic and cluster components in the laser-induced plumes on the plume dynamics and plasma shielding effect have not been studied yet theoretically.

*avolkov1@ua.edu; phone 1 205 348-4882; fax 1 205 348-6959; http://volkov.eng.ua.edu/index.html.

The goal of the present work is to develop a computational model for predicting the dynamics of ionization and radiation absorption in the two-phase plasma plumes induced by nanosecond laser pulses. This hybrid computational model, where the non-equilibrium collision-radiation plasma model for the atomic component is combined with the kinetic equation for the distribution function of cluster size and temperature, is then used to study the effects of various factors on plasma shielding in multi-phase plasma plumes induced by irradiation of a copper target by individual laser pulses.

2. COMPUTATIONAL MODEL

The computational model utilized in the present work to describe the formation and expansion of two-phase laser-induced plasma plumes includes three major components: (1) a thermal model of the irradiated target, which predicts the surface temperature and material removal rate, (2) a model of the gaseous plume, which describes its expansion, ionization, and absorption of laser radiation based on the collision-radiation plasma model, and (3) a cluster model that predicts sizes and temperatures of large clusters generated during fragmentation of the irradiated target. These components of the computational model are strongly coupled with each other. For computationally efficient simulations, this model is implemented in the form of a quasi-1D model, when the one-dimensional (1D) thermal model is combined with models of homogenous two-phase plumes.

2.1 Thermal model of the irradiated target

The thermal model of the irradiated target predicts the temperature distribution inside the target material. The 1D target temperature field $T_t(t,\xi)$ is described in a moving frame of reference with the coordinate $\xi=x-X_w(t)$, where t is the time, x is the coordinate in the laboratory frame of reference, counting along the normal to the irradiated surface from the point x=0 that corresponds to the initial position of the surface at t=0, and the interface function $X_w(t)$ is equal to the coordinate x of the surface at time t. The temperature field $T_t(t,\xi)$ and position of the surface $X_w(t)$ are determined by the equations

$$\rho_t[c_t + L_m \delta(T_t - T_m)] \left(\frac{\partial T_t}{\partial t} + V_w \frac{\partial T_t}{\partial \xi} \right) = \frac{\partial}{\partial \xi} \left(\kappa_t \frac{\partial T_t}{\partial \xi} \right) + (1 - R_t) \alpha_t I_w(t) \exp(-\alpha_t |\xi|), \tag{1}$$

$$\frac{dX_w}{dt} = -V_w,\tag{2}$$

where c_t , ρ_t , κ_t , α_t , R_t , L_m , and T_m are the specific heat, density, thermal conductivity, linear absorption coefficient, reflectivity, latent heat of melting, and melting temperature of the target material, V_w is the velocity of surface recession due to ablation of the target material, $I_w(t)$ is the intensity of laser radiation incident to the target, and $\delta(T)$ is the Dirac delta function. The term $L_m \delta(T_t - T_m)$ in Eq. (1) accounts for the energy required to melt or re-solidify the target material in the framework of the enthalpy formulation approach [11,12]. The last term on the right-hand side of Eq. (1) describes the absorption of laser radiation according to Beer's law. The local values of material properties c_t , ρ_t , and κ_t in Eq. (1), are calculated as functions of temperature by interpolating constant values specific for solid and liquid material [13].

The interface velocity $V_w = \psi_w/\rho_t$ is defined by the mass flux density ψ_w of the ablated material that is removed from the irradiated surface. The value of ψ_w includes contributions from normal evaporation, ψ_e , and volumetric boiling, ψ_{vb} :

$$\psi_w = \psi_e + \psi_{vb}. \tag{3}$$

The evaporation flux density ψ_e is calculated using the Hertz-Knudsen model [14] with the evaporation coefficient equal to 1 as

$$\psi_e = \frac{p_v(T_w)}{\sqrt{2\pi(k_B/m_a)T_w}},\tag{4}$$

where $T_w = T_t(t, 0)$ is the surface temperature, m_a is the mass of a vapor atom, k_B is the Boltzmann constant, and $p_v(T)$ is the saturated vapor pressure at temperature T which is determined by the Clausius-Clapeyron equation:

$$p_{\nu}(T) = p_{\nu,0} \exp\left[\frac{L_{\nu}}{k_B/m_a} \left(\frac{1}{T_{\nu,0}} - \frac{1}{T}\right)\right]. \tag{5}$$

In Eq. (5), L_v is the latent heat of boiling, and $T_{v,0}$ is the boiling temperature at pressure $p_{v,0}$. The volumetric boiling flux density ψ_{vb} is defined to ensure that the surface temperature does not exceed the threshold temperature for volumetric boiling T_{vb} , which is expected to be close to the thermodynamic critical temperature T_c . This can be achieved with

$$\psi_{vb} = \begin{cases} 0 & T_w < T_{vb}; \\ \rho_t \Gamma(T_w - T_{vb}) & T_w \ge T_{vb}, \end{cases}$$
 (6)

where the parameter Γ must be sufficiently large to enable almost immediate removal of the target material layer where the temperature is greater than T_{vb} .

Eq. (1) is solved in a domain of finite size H_t . At the initial time t=0, the target is assumed to have a uniform temperature T_0 , so that Eq. (1) and (2) are solved with the initial conditions $T_t(0,\xi) = T_0$ and $X_w(0) = 0$ at t=0. At the irradiated surface where $\xi = 0$, the boundary conditions for Eq. (1) represent an energy balance equation:

$$L_{\nu}^{*}(T_{w})\rho_{t}V_{w} = -\kappa_{t} \frac{\partial T_{t}}{\partial \xi} \Big|_{\xi=0}, \tag{7}$$

where $L_v^*(T_w)$ is the modified latent heat of boiling that approaches 0 when $T_w \to T_{vb}$. This quantity is defined as $L_v^*(T_w) = L_v$ at $T_w \le T_{vb,0}$ and $L_v^*(T_w) = 0$ at $T_w \ge T_{vb}$, while $L_v^*(T_w)$ smoothly varies between L_v and 0 as a cubic function when T_w varies between $T_{vb,0}$ and T_{vb} . The smooth transition of $L_v^*(T_w)$ to 0 ensures monotonic distribution of the material temperature near the surface at $T_w \ge T_{vb}$. The value of H_t is assumed to be sufficiently large, so that the variation of temperature at this boundary can be neglected during the whole process under consideration. Then the lower boundary of the computational domain at $\xi = -H_t$ can be assumed to be isothermal and kept at the initial target temperature T_0 .

The model of volumetric boiling in the form of Eq. (6) and (7) includes three parameters: T_{vb} , $T_{vb,0}$, and Γ . The results of simulations, however, only marginally depend on $T_{vb,0}$ and Γ if $T_{vb,0}$ is close to T_{vb} and Γ is sufficiently large. In the present work, all simulations are performed with $T_{vb,0} = 0.95T_{vb}$ and $\Gamma = 0.1 \text{ ms}^{-1}\text{K}^{-1}$.

2.2 Collision-radiation model of plasma plume

For modeling the two-phase plasma plume expansion into a vacuum, a quasi-1D model is used, where the expanding plasma plume is represented by a homogeneous plasma layer of thickness $\Delta(t)$ [15]. It is assumed that the gaseous component of the plume includes neutral vapor atoms, ions, and electrons. The thickness of the plasma layer $\Delta(t)$, the number density of ions n_n^z with charge z (z = 0, ..., Z) in the excited state n with energy E_n^z ($n = 0, ..., N^z$), as well as the electron, T_e , and ion, T_a , temperatures are determined by the equations:

$$\frac{d\Delta}{dt} = C_{PE} \sqrt{\frac{8k_B T_a}{\pi m_a}},\tag{8}$$

$$\frac{d(\Delta \cdot n_n^z)}{dt} = \Delta \cdot \left(R_{n,PI}^z \chi + R_{n,EI}^z + R_{n,EE}^z + R_{n,C}^z \right) + F_{n,W}^z, \qquad z = 0, \dots, Z, \ n = 0, \dots N^z,$$
 (9)

$$\frac{d(\Delta \cdot U_e)}{dt} = \Delta \cdot \left(Q_{e,PI} \chi - Q_{EI} - Q_{EE} - Q_{ea} + Q_{IB} \chi - Q_{BE} + Q_{e,C} \right) + 2k_B T_w F_{e,w},\tag{10}$$

$$\frac{d(\Delta \cdot U_a)}{dt} = \Delta \cdot \left(Q_{a,PI} \chi + Q_{EI} + Q_{EE} + Q_{ea} + Q_{a,C} \right) + \sum_{z=0}^{Z} \sum_{n=0}^{N^z} (2k_B T_w + E_n^z) F_{n,w}^z, \tag{11}$$

where $U_e = (3/2)k_BT_en_e$ and

$$U_a = \sum_{z=0}^{Z} \sum_{n=0}^{N^z} \left(\frac{3}{2} k_B T_a + E_n^z \right) n_n^z \tag{12}$$

are the densities of electron and ion internal energy; $R_{n,PI}^z$, $R_{n,EI}^z$, $R_{n,EI}^z$, $R_{n,E}^z$ are the kinetic rates that describe the change in ion densities due to photoionization (PI), electron ionization and recombination (EI), electron excitation and deexcitation (EE), and evaporation and condensation on cluster surfaces, respectively; $F_{n,w}^z$ and $F_{e,w}$ are the rates of change of the number of corresponding ions and electrons due to material removal from the irradiated surface; $Q_{e,PI}$ and $Q_{a,PI}$ are the rates of electron and ion energy changes due to PI; Q_{EI} , Q_{EE} , and Q_{ea} are energy exchange rates between electrons and ions due to EI, EE, and electrons-ion elastic collisions (EA), respectively; Q_{IB} and Q_{BE} are the rates of energy absorption and emission in inverse bremsstrahlung and bremsstrahlung, respectively; $Q_{e,C}$ and $Q_{a,C}$ are the rates of electron and ion

energy changes due to evaporation and condensation on cluster surfaces; $\chi = (1 - \exp(-\alpha_p \Delta))/(\alpha_p \Delta)$ is the laser radiation extinction factor; and α_P is the total linear extinction coefficient of the two-phase plasma plume. The number density of electrons n_e and $F_{e,w}$ are determined by the condition of quasi-neutrality of plasma:

$$n_e = \sum_{z=1}^{Z} \sum_{n=0}^{N^z} z \, n_n^z, \tag{13}$$

$$F_{e,w} = \sum_{z=1}^{Z} \sum_{n=0}^{N^{z}} z \, F_{n,w}^{z} \,. \tag{14}$$

The coefficient C_{PE} in Eq. (8) can be used to fit the results obtained with this quasi-1D model to the known simulations, where the actual expansion dynamics and non-homogeneous distribution of plume parameters are accounted for. The comparison of the results obtained with the presented model and 1D kinetic simulations of quasi-equilibrium laser-induced plasma plumes [13,16] showed that the best agreement is achieved when C_{PE} varies from 1 to 3 (for this comparison, Eq. (9) was replaced by the calculation of ion population densities based on the Saha equations of ionization equilibrium). The preliminary parametric study, performed in the present work, where C_{PE} was varied in that range, showed that the qualitative conclusions about the effect of clusters on parameters of the gaseous component and shielding effect do not depend on C_{PE} . Therefore, all computational results that are further discussed in Section 3 are obtained at $C_{PE} = 1$.

The calculations based on Eq. (9)-(11) are performed using the coarse-grained (CG) energy spectra of ions. The coarse-graining is performed by keeping all energy levels with $E_n^z < E_0^z + \Delta E_0$ unchanged, while all other levels are grouped into bins of size ΔE in the energy space. Then all levels belonging to the same bin are replaced by a single CG level with average parameters. The details of the coarse-graining procedure, which is completely defined by two parameters, ΔE_0 and ΔE , will be described elsewhere [17]. After coarse-graining, all rates in Eq. (9)-(11), except for PI rates, are determined assuming that the rate equations established for the true energy spectrum can be used without changes for the CG spectrum. A parametric study of plasma plume expansion, where ΔE_0 and ΔE were varied in broad ranges, was performed. This study confirmed that a good accuracy of simulations based on this simple approach can be achieved at a reasonably small ΔE_0 and large ΔE . This makes the simulations based on the collision-radiation model computationally efficient.

The rates of EI, EE, and EA processes are calculated based on the models used in Ref. [15]. The rates of radiation processes Q_{IB} and Q_{BE} are calculated in the form used in Ref. [16,18,19]. The rates of mass and energy exchange between gaseous components of the plume and clusters, $R_{n,C}^z$, $Q_{e,C}$, and $Q_{a,C}$, are considered in Section 2.3. The ion evaporation rates on the target surface $F_{n,w}^z$ are defined assuming that the mass fraction of clusters in the ablation flux is equal to $\beta_C(T_w)$, so that the total number flux of ions and atoms from the surface is equal $[1 - \beta_C(T_w)]\psi_w/m_a$. The evaporated fractions of ions with various z and n are found from the Saha-Boltzmann equilibrium at the surface temperature T_w and saturated vapor pressure $p_v(T_w)$ (Eq. (5)). It is assumed that the clusters are emitted from the surface only under conditions of volumetric boiling, so $\beta_C(T_w) = \beta_C = const$ at $T_w \ge T_{vb}$ and $\beta_C(T_w) = 0$ at $T_w < T_{vb}$.

The calculations of the PI rates $R_{n,PI}^z$ for the CG spectrum require special treatment. For the true energy spectrum, the PI rates are calculated in the form adopted from Ref. [16,20]. The calculation of CG $R_{n,PI}^z$ is based on the quasi-equilibrium coarse-graining, which is similar to the Boltzmann coarse-graining, e.g., [21,22]. Namely, the values of $R_{n,PI}^z$ are obtained by the summation of the contributions of individual levels of true spectrum belonging to the corresponding bin of the CG spectrum assuming equilibrium Boltzmann distribution of relative population densities within the bin. To make this approach computationally efficient, the obtained temperature-dependent rate coefficients were pre-calculated and then obtained by interpolation in the look-up tables during simulations. The details of this approach will be described elsewhere [17].

The intensity of laser radiation incident to the surface, $I_w(t)$ in Eq. (1), is defined by Beer's law as $I_w(t) = I_0(t) \exp(-\alpha_P \Delta)$, where $I_0(t)$ is the incoming laser intensity, and the total linear extinction coefficient of the two-phase plume α_p is equal to

$$\alpha_P = \alpha_{PI} + \alpha_{IB} + \alpha_{CA} + \alpha_{C.S}. \tag{15}$$

In Eq. (15), $\alpha_{PI} = Q_{PI}/I_0(t)$, $\alpha_{IB} = Q_{IB}/I_0(t)$, while $\alpha_{C,A}$ and $\alpha_{C,S}$ account for absorption and scattering of laser radiation by clusters as described in Section 2.3.

2.3 Kinetic equation for clusters and droplets

It is assumed that each cluster is a sphere of radius r_p and temperature T_p . The distribution of cluster radii and temperatures in the homogeneous quasi-1D plasma plume is described by the distribution function $f_p(r_p, T_p, t)$ normalized by the number density of clusters n_p :

$$n_p(t) = \int_0^\infty \int_0^\infty f_p(r_p, T_p, t) dr_p dT_p.$$
 (16)

Since the major focus of the present work is on the effects related to the generation of large clusters at the fragmentation of the irradiated target, the nucleation of small atomic clusters in the plume is not considered. In addition, the deposition of clusters back to the irradiated surface is neglected. Then the variation of $f_p(r_p, T_p, t)$ in time is described by the kinetic equation in the phase space of variables r_p and T_p :

$$\frac{\partial}{\partial t} (\Delta f_p) + \Delta \left[\frac{\partial}{\partial r_p} (\dot{r}_p f_p) + \frac{\partial}{\partial T_p} (\dot{T}_p f_p) \right] = I_{C,w}, \tag{17}$$

where \dot{r}_p and \dot{T}_p are rates of change of particle radius and temperature due to the mass and energy exchange with the surrounding gaseous plasma, and $I_{C.W}$ is the term describing the generation of new particles at the irradiated surface.

The values of \dot{r}_p and \dot{T}_p are determined by the equation of mass and energy exchange for an individual cluster:

$$\frac{dm_p}{dt} = \Psi_{GP},\tag{18}$$

$$\frac{dm_p}{dt}(c_p m_p T_p) = Q_{GP} + L_p \Psi_{GP} + \sigma_{p,A} I_0 \chi, \tag{19}$$

where $m_p = (4/3)\pi r_p^3 \rho_p$, ρ_p is the cluster mass, c_p , and L_p are the density, specific heat, and latent heat of vaporization of the cluster material, Ψ_{GP} is the mass flux at the cluster surface due to its evaporation and condensation of the surrounding vapor, Q_{GP} is the energy flux to the cluster from surrounding gas, and $\sigma_{p,A}$ is the cluster absorption cross-section. The cluster generation term can be written in the form

$$I_{C,w}(r_p, T_p, t) = \beta_C \frac{\psi_w(t)}{\langle m_p \rangle_w} f_{r,w}(r_p, t) f_{T,w}(T_p, t),$$
(20)

where $f_{r,w}(r_p,t)$ is the probability density function (PDF) of radii r_p of clusters generated at the surface, $f_{T,w}(T_p,t)$ is the PDF of temperatures T_p of clusters generated at the surface, and $\langle m_p \rangle_w$ is the average mass of the clusters emitted from the surface. Since the size and temperature distributions of clusters generated at volumetric boiling as functions of the thermal state of the target are currently unknown, it is assumed that $f_{r,w}(r_p,t)$ is given by the Weibull distribution with constant mean r_W and standard deviation Δr_w , while $f_{T,w}(T_p,t)$ is given by the Gaussian distribution with the mean equal to $T_w(t)$ and constant standard deviation $\Delta T_w \ll T_w$. The values of r_w , Δr_w , and ΔT_w are considered as the model parameters.

The mass flux Ψ_{GP} is determined using the Hertz-Knudsen model adopted for the evaporation and condensation of clusters surrounded by vapor [23] with the evaporation and condensation coefficients equal to 1. The value of Q_{GP} is determined based on the approximation of the Nusselt number for spherical particles which was obtained in Ref. [24] and accounts for the rarefaction of the gas around the particle. The term Q_{GP} also includes a contribution of kinetic energy carried by atoms leaving the cluster surface and deposited on it. The cluster total absorption cross-section, $\sigma_{p,A} = \sigma_{p,A}(r_p, \lambda_L)$, and scattering cross-section, $\sigma_{p,S} = \sigma_{p,S}(r_p, \lambda_L)$, (λ_L is the laser wavelength) are determined based on the Mie theory [25]. All physical properties of the cluster material are assumed to be equal to the properties of the target material in the liquid state.

If the physical quantity $\phi_p = \phi_p(r_p, T_p, t)$ is associated with an individual cluster, then the density of this quantity per unit volume of the plume is equal to

$$\langle \phi_p \rangle (t) = \int_0^\infty \int_0^\infty \phi_p(r_p, T_p, t) f_p(r_p, T_p, t) dr_p dT_p.$$
 (21)

Then, in Eq. (15), $\alpha_{C,A} = \langle \sigma_{p,A} \rangle$ and $\alpha_{C,S} = \langle \sigma_{p,S} \rangle$. To define the cluster-gas coupling terms in Eq. (9)-(11), it is additionally assumed that the fractions of ions and atoms with various z and n are determined by the Saha-Boltzmann equilibrium distributions at the average cluster temperature $[T_p] = \langle m_p T_p \rangle / \langle m_p \rangle$ and saturated vapor pressure $p_v([T_p])$, while the total evaporation rate in a unit volume is equal to $-\langle \Psi_{GP} \rangle / m_a$. Then $Q_{e,C}$ in Eq. (10) is determined by the average kinetic energy of electrons emitted from the cluster surface at temperature $[T_p]$ and condition of quasi-neutrality of plasma.

2.4 Simulation parameters

The simulations are performed for a copper target at an initial temperature of $T_0 = 300$ K irradiated by a pulsed laser at a wavelength of 266 nm. The physical properties of the target and cluster material are adopted from Ref. [13]. The energy spectra of Cu atoms and for z = 0, ..., Z = 3 are taken from the NIST database [26,27]. The CG energy spectra of Cu atoms and ions are obtained at $\Delta E_0 = 5$ eV, $\Delta E = 1$ eV, and contains a total of 61 energy levels. The refractive index of Cu, which is required for calculations of the Mie cross-sections, is taken from Ref. [28]. Other properties of Cu atoms and ions required for calculations of individual rates in Eq. (9)-(11) are taken from Ref. [15,16]. The thermal conductivity of Cu vapor as a function of temperature, which is required to find Q_{GP} , is determined by the power-law dependence obtained in Ref. [29] based on the quantum mechanical calculations of the potential energy of Cu-Cu atom pairs. The threshold temperature for volumetric boiling T_{vb} is assumed to be equal to $0.9T_c$ [3], where $T_c = 8280$ K is the critical temperature for Cu [30]. The parameter ΔT_w in Eq. (20) is equal to 100 K, while $\Delta r_w = r_w/2$. The values of r_w and β_C are varied in simulations.

A single pulse of incident laser radiation with a duration of $\tau_L = 10$ ns is assumed to have the smoothed flat-top temporal shape, with the intensity given by the equation

$$I_{0}(t) = \frac{F_{L}}{\tau_{L} - \tau_{S}} \begin{cases} 0, & t \leq 0 \text{ or } t \geq \tau_{L}; \\ \frac{1}{2} \left[1 + \sin\left(\frac{\pi t}{\tau_{S}} - \frac{\pi}{2}\right) \right], & t < \tau_{S}; \\ 1, & \tau_{S} \leq t \leq \tau_{L} - \tau_{S}; \\ \frac{1}{2} \left[1 - \sin\left(\frac{\pi (t + \tau_{S} - \tau_{L})}{\tau_{S}} - \frac{\pi}{2}\right) \right], & t > \tau_{L} - \tau_{S}, \end{cases}$$
(22)

where F_L is the laser fluence of a single pulse, and $\tau_S = 1$ ns is the pulse smoothing time. The value of F_L is varied in simulations.

3. RESULTS AND DISCUSSION

The preliminary simulations were performed for a range of laser fluence F_L from 4 Jcm⁻² to 12 Jcm⁻². These simulations showed that, with increasing F_L above the threshold for volumetric boiling, the effects of clusters on the plume parameters and degree of plasma shielding become gradually stronger, but the variation of F_L does not induce qualitative changes in the variation of plume parameters. Therefore, the major results obtained in the present work are illustrated with a single case of $F_L = 9$ Jcm⁻², which corresponds to a moderate degree of plasma shielding.

The major goal of simulations was to reveal the effects of various assumptions about the cluster generation process at the irradiated surface as well as the mass and energy exchange between gaseous component of the plume and clusters on the plume parameter, degrees of ionization and plasma shielding, and total ablation depth. To perform such a methodological study, four options for modeling volumetric boiling and cluster generation are considered: Model I with no volumetric boiling and no clusters ($\psi_{vb} = 0$ in Eq. (3) and $\beta_C = 0$); model II with volumetric boiling without clusters ($\beta_C = 0$); model III with volumetric boiling and model IV where volumetric boiling is accounted for in full and $\beta_C = 0.7$. A summary of the distinctive features of these models is provided in Table 1. The results of these simulations are illustrated in Fig. 1-3. In these simulations, the average size r_w of clusters generated at the surface is equal to 200 nm.

Table 1. Distinctive features of the models used in the present work.

Model	Collision-radiation model for gaseous plasma	Volumetric boiling	Mass fraction of clusters in the ablated material flux β_C	Clusters present in the plume
I	Yes	No	0	No
II	Yes	Yes	0	No
III	Yes	Yes	0.7	No
IV	Yes	Yes	0.7	Yes

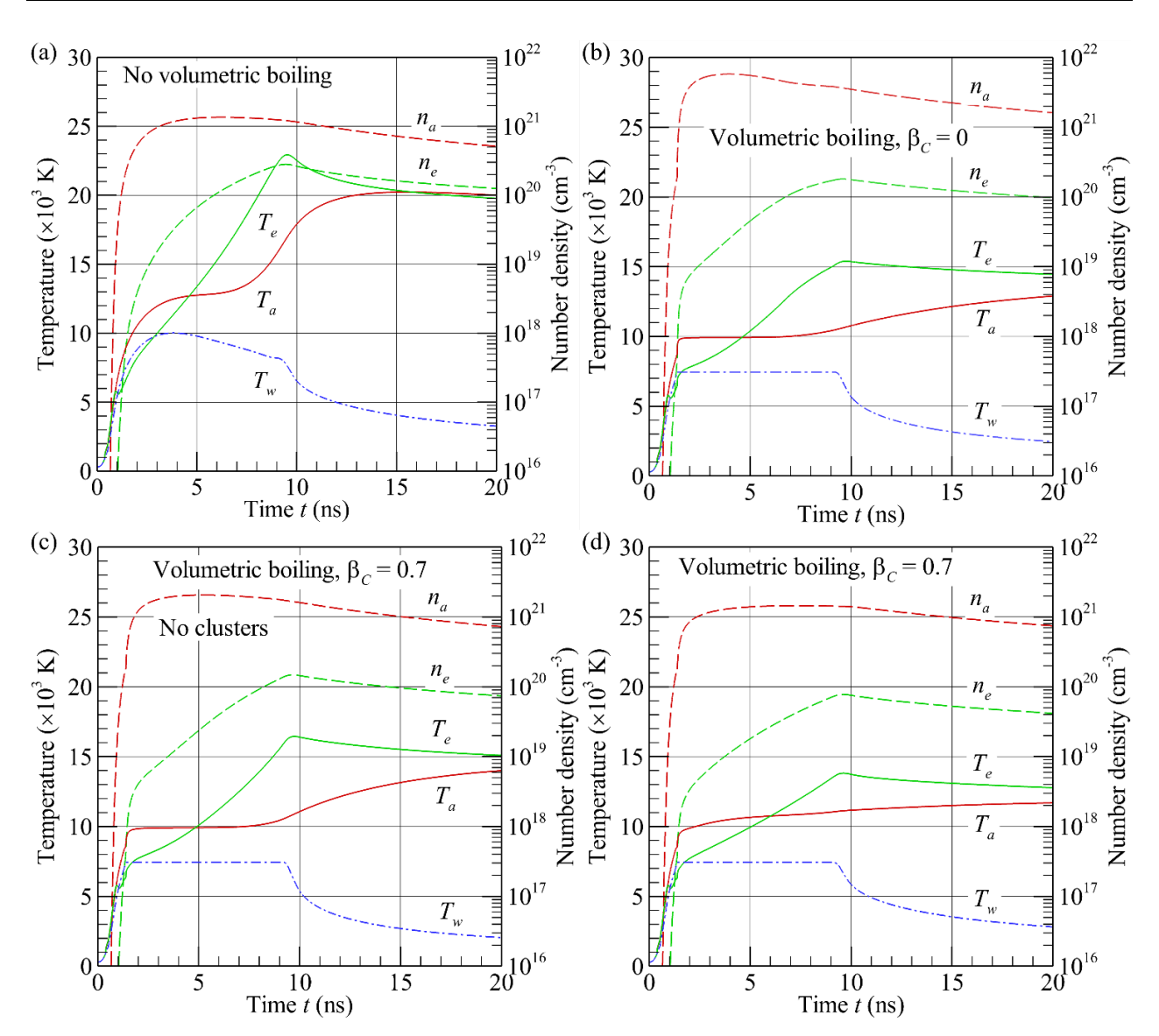


Figure 1. Ion temperature T_a (solid red curves), electron temperature T_e (solid green curves), surface temperature T_w (dashed-dotted blue curves), number density of ions and neutral atoms n_a (dashed red curves), and electron number density n_e (dashed green curves) versus time t obtained with models I (a), II (b), III (c), and IV (d) at $F_L = 9$ Jcm⁻² and $r_w = 200$ nm. The simulations based on models III and IV are performed at $\beta_C = 0.7$.

The largest electron, T_e , and ion, T_a , temperatures as well as the relative fraction of electrons compared to heavy particles n_e/n_a are observed in the simulation based on model I, when the volumetric boiling is not accounted for (Fig. 1(a)). The maximum number density of neutral atoms and ions, as expected, is observed in the simulation based on model II, when

the volumetric boiling is accounted for without the generation of clusters (Fig. 1(b)). In terms of maximum densities and temperature, model III is an intermediate model between models I and II (Fig. 1(c)). The results based on model IV, when the presence of clusters in the plume is accounted for, are characterized by the minimum temperatures, T_e and T_a , in the plume and minimum degree of the ionization at the end of the laser pulse (Fig. 1(d)). Overall, the simulations reveal only moderate differences between the parameters of the gaseous component of the plume obtained using models III and IV. Practically, it means that, if a computation model cannot account for the presence of clusters and interphase mass and energy exchange, the most accurate predictions of the gaseous plasma parameters can be obtained if the flux of the ablated material accounts for the volumetric boiling at realistic mass fraction of clusters.

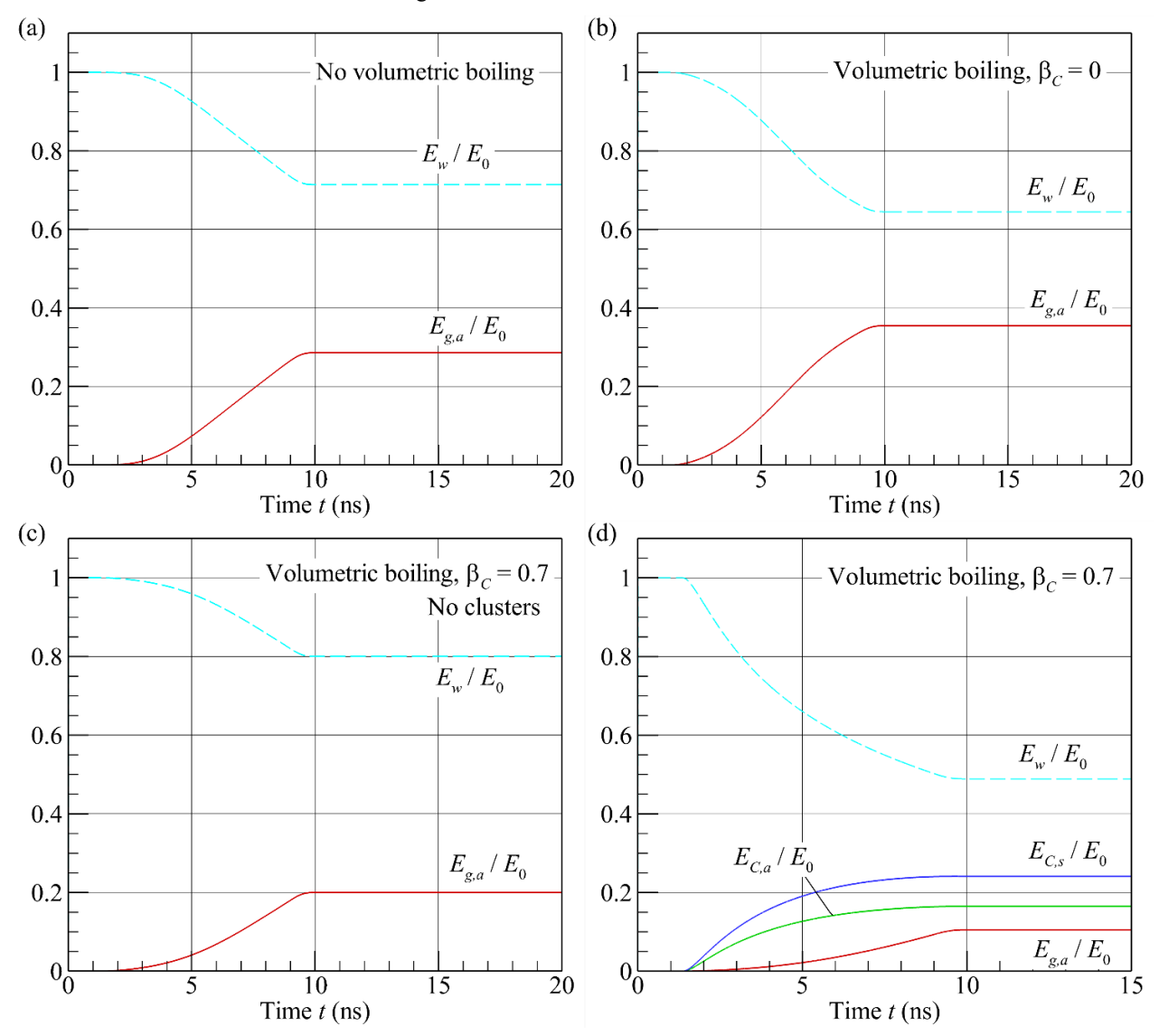


Figure 2. Relative laser energy flux absorbed by the gaseous phase $E_{g,a}/E_0$ (solid red curves), absorbed by clusters $E_{C,a}/E_0$ (solid green curve), scattered by clusters $E_{C,s}/E_0$ (solid blue curve), and incident to the irradiated surface E_w/E_0 (dashed cyan curves) versus time t obtained with models I (a), II (b), III (c), and IV (d) at $F_L = 9$ Jcm⁻² and $r_w = 200$ nm. The simulations based on models III and IV are performed at $\beta_C = 0.7$.

To characterize the absorption and scattering of laser radiation by the two-phase plumes, the ratios of instant energy fluxes absorbed by gas, $E_{g,a}(t)$, absorbed by clusters $E_{C,a}(t)$, and scattered by clusters, $E_{C,s}(t)$, to the laser energy flux

$$E_0(t) = \int_0^t I_0(\bar{t}) d\bar{t}$$
 (23)

were calculated (Fig. 2). The laser energy flux received by the target is equal to $E_w(t) = E_0(t) - (E_{g,a}(t) + E_{C,a}(t) + E_{g,s}(t))$. The maximum degree of plasma shielding is realized in simulations with model II, where the volumetric boiling is taken into account but the whole ablation flux consists of atomic vapor (Fig. 2(b)). When the clusters are present in the two-phase plume, the leading mechanism of the laser radiation extinction is the scattering of light by clusters, while the absorption by the gaseous plasma provides the smallest contribution. Despite the quantitative similarity between temperatures and densities of the gaseous component obtained with models III and IV (Fig. 1(b, c)), the degree of plasma shielding measured by $1 - E_w(\tau_L)/E_0(\tau_L)$ is more than twice larger in the case of model IV compared to model III.

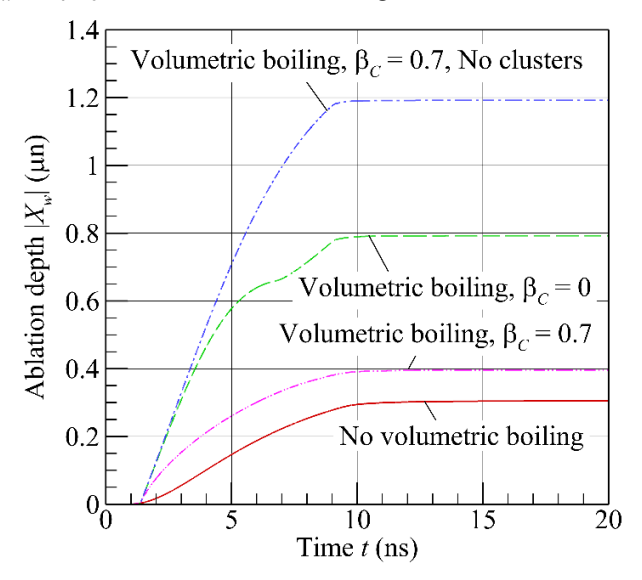


Figure 3. Ablation depth $|X_w|$ versus time t obtained with models I (solid red curve), II (dashed green curve), III (dashed-dotted blue curve), and IV (dashed-dotted magenta curve) at $F_L = 9$ Jcm⁻² and $r_w = 100$ nm. The simulations based on models III and IV are performed at $\beta_C = 0.7$.

The generation of clusters at the target material fragmentation also strongly affects the total ablation depth (Fig. 3). The minimum ablation depth is predicted by model I, where the volumetric boiling is not accounted for. The maximum ablation depth is realized in the simulation based on model III, where the plasma shielding effect is minimal. When the scattering and absorption of laser radiation by clusters and interphase mass and energy exchange are accounted for (model IV), the ablation depth becomes ~3 times smaller compared to model III. Thus, the relatively good agreement between models III and IV in terms of the gaseous plasma parameters in Fig. 1 is not translated into a good agreement between these two cases in terms of the alation depth primarily because the absorption and scattering of laser radiation by clusters strongly affects the total degree of radiation attenuation by the two-phase plume.

The mass fraction of clusters in the plume $c_C = \rho_C/(\rho_C + \rho_a)$ (here, ρ_a and ρ_C are the mass densities of the atomic component and clusters in the plume, respectively) strongly reduces in time. By the end of the plume, c_C can be a few times smaller than β_C (Fig. 4). This highlights a very strong effect of interphase mass transfer from clusters to the gas phase during the laser pulse. The large evaporation rate is supported by the laser heating of clusters, so that the mass fraction of clusters reduces much slower after termination of the laser pulse. With the reduction of the average radius of clusters generated at the target surface from 200 nm to 50 nm, c_C at the end of the pulse reduces from \sim 0.22 to \sim 0.03. The strong evaporation from clusters has important consequences for the total degree of plasma shielding. On one hand, cluster evaporation reduces the total amount of energy that can be absorbed and scattered by clusters. On the other hand, it delays the onset of strong ionization in the gaseous plume, so that the absorption by the gaseous plasma in the two-phase plume becomes weaker than in the plume, where all material is assumed to be ablated in the form of atomic vapor.

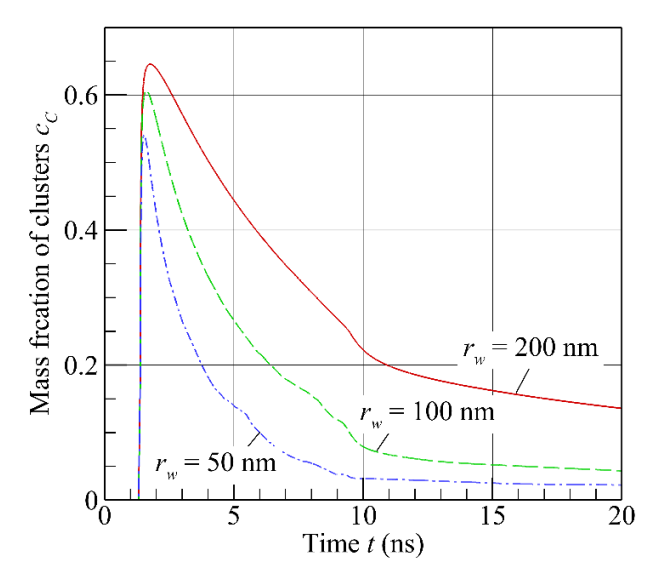


Figure 4. Mass fraction of clusters in the plume c_C versus time t obtained with model IV at $F_L = 9$ Jcm⁻² and $\beta_C = 0.7$ for $r_w = 200$ nm (solid red curve), 100 nm (dashed green curve), and 50 nm (dashed-dotted blue curve).

It is worth noting that the results of the modeling of two-phase laser-induced plasma plumes can be sensitive to certain model assumptions. An example of such sensitivity is given by the model of high-temperature vaporization of clusters. All results shown in Fig. 1-4 are obtained assuming equilibrium ionization of vapor emitted from the cluster surface at the average cluster temperature and corresponding saturated vapor pressure. At the same time, the process of emission of charged particles that accompanies the strong vaporization of small clusters at relatively large temperatures is not well understood. As an alternative to the model of equilibrium ionization, one can assume that only neutral atoms in the ground energy state are emitted from the cluster surface, so that $F_{0,w}^0 = -\langle \Psi_{GP} \rangle/m_a$, $F_{n,w}^z = 0$ when n > 0 or z > 0, $Q_{e,C} = 0$, and $Q_{a,C} = -\langle Q_{GP} \rangle$. The variation of the plume parameters obtained in the simulations based on model IV and this assumption is illustrated in Fig. 5. These results can be compared with the corresponding results obtained with the assumption of equilibrium ionization, which are shown in Fig. 1(d) and 2(d). The total degrees of plasma shielding in both cases are close to each other due to the dominant contribution of scattering by clusters. At the same time, the assumption of emission of only neutral atoms reduces the relative density of electrons n_e/n_a in about two orders of magnitude to ~ 0.002 , while the electron temperature remains at a level of the threshold temperature T_{vb} . As a result, the contribution of absorption of laser radiation by the gaseous component, $E_{g,a}/E_0$, becomes marginally small.

4. CONCLUSIONS

The developed computational model enables simulations of two-phase gas-cluster non-equilibrium plasma plumes induced by irradiation of a metal target with nanosecond laser pulses. The model accounts for the generation of large clusters due to fragmentation of the irradiated surface and all-way coupling between the atomic component of the plume, clusters, and radiation. Due to the assumption of a homogeneous distribution of plume parameters, the computations based on this model are relatively fast. This opens opportunities for parametric studies of the effect of plasma shielding in a multidimensional parameter space in engineering applications.

The results of simulations obtained with this model indicate that the leading mechanism of laser attenuation in the two-phase plumes induced by nanosecond laser pulses in the regime of volumetric boiling is the scattering of laser radiation by clusters. The degree of attenuation of the laser radiation due to its absorption and scattering by clusters can be a few times larger than the degree of absorption by the gaseous component of the two-phase plume. The simulations also reveal very strong evaporation of clusters during the laser pulse, which is supported by the absorption of laser radiation by clusters. At the end of the pulse, due to cluster evaporation, the plume mostly consists of atomic components, even if the clusters dominate the flux of the ablated material. In the range of parameters considered in simulations, a decrease in the average cluster size in the ablation flux increases the rate of cluster evaporation and reduces the mass fraction of clusters in the plume by the end of the laser pulse.

The developed model can be generalized for predicting the effect of clusters on the plasma shielding in plumes induced by individual ultrashort laser pulses and bursts of pulses with high intra-burst repetition rates. The prediction of the plasma shielding effect under conditions of burst laser ablation is the subject of the author's current work.

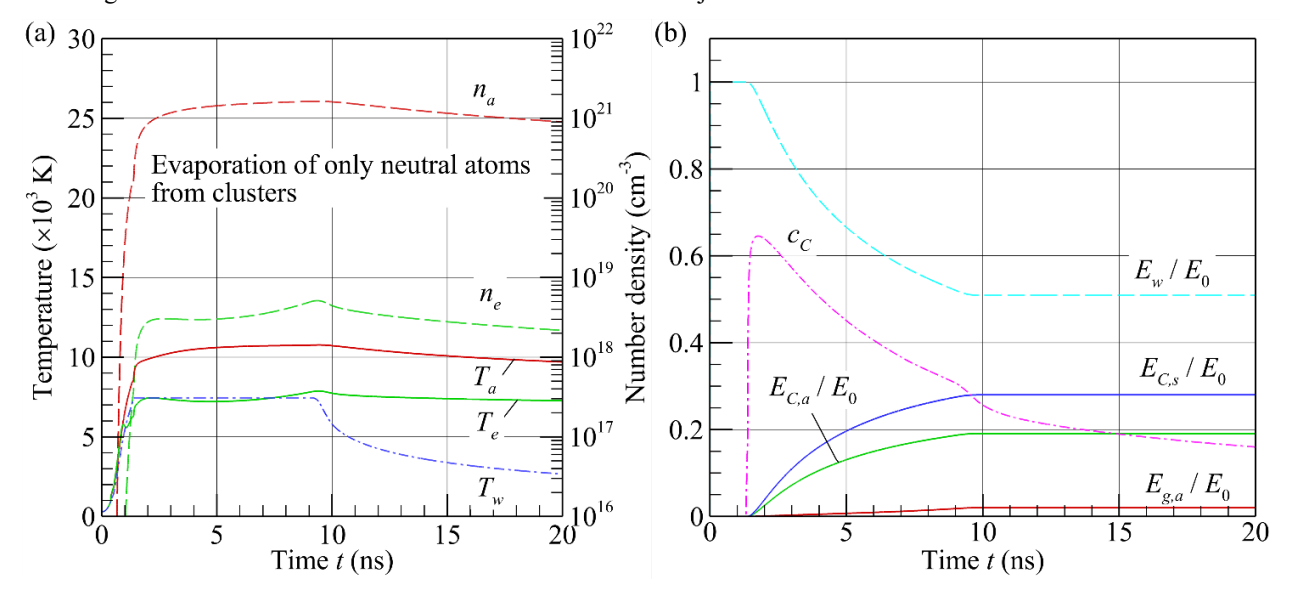


Figure 5. (a), ion temperature T_a (solid red curve), electron temperature T_e (solid green curve), surface temperature T_w (dashed-dotted blue curves), number density of ions and neutral atoms n_a (dashed red curve), and electron number density n_e (dashed green curve) versus time t; (b), relative laser energy flux absorbed by the gaseous phase $E_{g,a}/E_0$ (solid red curve), absorbed by clusters $E_{C,a}/E_0$ (solid green curve), scattered by clusters $E_{C,s}/E_0$ (solid blue curve), and incident to the irradiated surface E_w/E_0 (dashed cyan curve), as well mass fraction of clusters in the plume c_C (dashed-dotted magenta curve) versus time t. These results are obtained using model IV at $F_L = 9 \, \mathrm{Jcm}^{-2}$, $r_w = 200 \, \mathrm{nm}$, and $\beta_C = 0.7 \, \mathrm{with}$ the additional assumption that only neutral atoms are evaporated from clusters.

ACKNOWLEDGEMENTS

This work was supported by the National Science Foundation (USA) through RII-Track-1 Future Technologies and Enabling Plasma Processes project (award OIA-2148653).

REFERENCES

- [1] J.H. Yoo, S.H. Jeong, X.L. Mao, R. Greif, R.E. Russo, "Evidence for phase-explosion and generation of large particles during high power nanosecond laser ablation of silicon," *Appl. Phys. Lett.* **76**, 783-785 (2000).
- [2] C. Pornealla, D.A. Willis, "Observation of nanosecond laser-induced phase explosion in aluminum," *Appl. Phys. Lett.* **89**, 211121 (2006).
- [3] R. Kelly, A. Miotello, "Comments on explosive mechanisms of laser sputtering," *Appl. Surf. Sci.* **96-98**, 205–215 (1996).
- [4] J.A. Aguilera, C. Aragóna, F. Peñalba, "Plasma shielding effect in laser ablation of metallic samples and its influence on LIBS analysis," *Appl. Surf. Sci.* **127-128**, 309-314 (1998).
- [5] D. Lacroix, G. Jeandel, C. Boudot, "Solution of the radiative transfer equation in an absorbing and scattering Nd:YAG laser-induced plume," *J. Appl. Phys.* **84**, 2443-2449 (1998).
- [6] A.A. Ionin, S.I. Kudryashov, L.V. Seleznev, "Near-critical phase explosion promoting breakdown plasma ignition during laser ablation of graphite," *Phys. Rev. E* **82**, 016404 (2010).
- [7] C. Wu, L.V. Zhigilei, "Microscopic mechanisms of laser spallation and ablation of metal targets from large-scale molecular dynamics simulations," *Appl. Phys. A* **114**, 11 (2014).
- [8] N. Farid, S.S. Harilal, H. Ding, A. Hassanein, "Emission features and expansion dynamics of nanosecond laser ablation plumes at different ambient pressures," *J. Appl. Phys.* **115**, 033107 (2014).
- [9] A.C. Forsman, P.S. Banks, M.D. Perry, E.M. Campbell, A.L. Dodell, M.S. Armas, "Double-pulse machining as a technique for the enhancement of material removal rates in laser machining of metals," *J. Appl. Phys.* **98**, 033302 (2005).

- [10] B. Bornschlegel, J. Finger, "In-situ analysis of ultrashort pulsed laser ablation with pulse bursts," *J. Laser Micro/Nanoeng.* **14**, 88–94 (2019).
- [11] W.D. Bennon, F.P. Incropera, "A continuum model for momentum, heat, and species transport in binary solid-liquid phase change systems I. Model formulation," *Int. J. Heat Mass Transfer* **30**, 2161-2170 (1987).
- [12] N.M. Bulgakova, R. Stoian, A. Rosenfeld, I.V. Hertel, W. Marine, E.E.B. Campbell, "A general continuum approach to describe fast electronic transport in pulsed laser irradiated materials: The problem of Coulomb explosion," *Appl. Phys.* A. **81**, 345-356 (2005).
- [13] O.A. Ranjbar, Z. Lin, A.N. Volkov, "One-dimensional kinetic simulations of plume expansion induced by multipulse laser irradiation in the burst mode at 266 nm wavelength," *Vacuum* **157**, 361–375 (2018).
- [14] C. Cercignani, Rarefied Gas Dynamics: From Basic Concepts to Actual Calculations (Cambridge University Press, 2000).
- [15] V. Morel, A. Bultel, B.G. Chéron, "Modeling of thermal and chemical non-equilibrium in a laser-induced aluminum plasma by means of a collisional-radiative model," *Spectrochimica Acta Part B* **65**, 830-841 (2010).
- [16] O.A. Ranjbar, Z. Lin, A.N. Volkov, "Effect of the spot size on ionization and degree of plasma shielding in plumes induced by irradiation of a copper target by multiple short laser pulses," *Appl. Phys. A* **126**, 355 (2020).
- [17] M.A. Stokes, A.N. Volkov, S.A. Khairallah, A.M. Rubenchik, Z. Lin, "A kinetic-continuum method combining the direct simulation Monte-Carlo with equilibrium and non-equilibrium ionization models for simulations of laser-induced plasma plumes" (in preparation).
- [18] M. Stokes, O. A. Ranjbar, Z. Lin, A. N. Volkov, "Expansion dynamics and radiation absorption in plumes induced by irradiation of a copper target by single and multiple nanosecond laser pulses in the doughnut beam mode," *Spectrochimica Acta Part B* 177, 106046 (2021).
- [19] A.N. Volkov, "Splitting of laser-induced neutral and plasma plumes: hydrodynamic origin of bimodal distributions of vapor density and plasma emission intensity," *J. Phys. D: Appl. Phys.* **54**, 37LT01 (2021).
- [20] D. Autrique, V. Alexiades, "Comment on "Laser ablation of Cu and plume expansion into 1 atm ambient gas" [J. Appl. Phys. 97, 063305 (2005)]," J. Appl. Phys. 115, 166101 (2014).
- [21] H.P. Le, A.R. Karagozian, J.-L. Cambier, "Complexity reduction of collisional-radiative kinetics for atomic plasma," *Phys. Plasmas* **20**, 123304 (2013).
- [22] R.J.E. Abrantes, A.R. Karagozian, D. Bilyeu, H.P. Le, "Complexity reduction effects on transient, atomic plasmas," *J. Quant. Spectrosc. Radiat. Transf.* **261**, 47-55 (2018).
- [23] A.H. Persad, C.A. Ward, "Expressions for the evaporation and condensation coefficients in the Hertz-Knudsen relation," *Chem. Rev.* **116**, 7727–7767 (2016).
- [24] L.L. Kavanau, "Heat transfer from spheres to a rarefied gas in subsonic flow," Trans. ASME 77, 617–623 (1955).
- [25] C.F. Bohren, D.R. Huffman, Absorption and Scattering of Light by Small Particles (Wiley, 1983).
- [26] J. Sugar, A. Musgrove, "Energy levels of copper, Cu I through Cu XXIX," J. Phys. Chem. Ref. Data 19, 527-616 (1990).
- [27] A. Kramida, Y. Ralchenko, J. Reader, NIST ASD Team, "NIST atomic spectra database (ver. 5.9) [Online]," National Institute of Standards and Technology, Gaithersburg, MD (2021).
- [28] P.B. Johnson, R.W. Christy, "Optical constants of the noble metals," *Phys. Rev. B* 6, 4370-4379 (1972).
- [29] K.W. Kayang, A.N. Volkov, P.A. Zhilyaev, F. Sharipov, "The ab initio potential energy curves of atom pairs and transport properties of high-temperature vapors of Cu and Si and their mixtures with He, Ar, and Xe gases," *Phys. Chem. Chem. Phys.* **25**, 4872–4898 (2023).
- [30] M. Aghaei, S. Mehrabian, S.H. Tavassoli, "Simulation of nanosecond pulsed laser ablation of copper samples: A focus on laser induced plasma radiation," *J. Appl. Phys.* **104**, 053303 (2008).